

Antibacterial activity of biosynthesized ZnO nanoflakes using Pandanus tectorius leaf extracts

S. S. Florence^{a,*}, C. Manna^a, K. Prabha^b, M. Bakri^c, R. A. Hagazy^c,
M. Sowjanya^d, M. Shariq^a

^aDepartment of Physics, Jazan University, Jizan, Saudi Arabia.

^bDepartment of Physics, Mother Teresa Women's University, Kodaikanal, Tamilnadu, India.

^cDepartment of Biology, Jazan University, Jizan, Saudi Arabia.

^dCenter of Nanotechnology, Indian Institute of Technology, Roorkee, India

The crystalline structure and morphology of semiconductor nanoparticles are important factors for determining their optical properties. To synthesis such nanoparticles, green synthesis is one of the most popular methods. In these green synthesis procedures, the plant extracts can be added to control the growth and particle size. In this present work, ZnO nanoflakes are synthesized in a cost-effective green synthesis method using pandanus tectorius leaf extract. The structure and morphology of as synthesized ZnO nanoflakes have been characterized by X-ray diffraction (XRD), Raman Spectroscopy, scanning electron microscopy (SEM), photoluminescence (PL) spectrophotometry and transmission electron microscopy (TEM). The SEM and TEM images reveal the formation of ZnO nanoflakes. The hexagonal wurtzite structure has been predicted from XRD results. Strong blue absorption and the enhanced luminescence property with respect to bulk have been observed from PL studies.

(Received January 18, 2022; Accepted 16 May, 2022)

Keywords: Semiconductors, Antimicrobial activities, Raman, X-ray techniques, Nanoparticles

1. Introduction

Recently, Metal oxide nanoparticles using cost-effective green synthesis has been preferred by the researchers of multidisciplinary fields including biology, chemistry, physics, materials science, and engineering. Among all metal oxide nanoparticles, zinc oxide nanoparticles are more familiar due to its high temperature endurance, high catalytic efficiency and antimicrobial properties. Among all these applications, antimicrobial studies of metal oxide nanomaterials are more significant due to the biggest challenges of microbial infections and resistance to antibiotic drugs which threaten the health of societies. Over the last three decades, the antimicrobial resistance related infections has increased dramatically. To overcome the phenomenon of multiple drug resistance (MDR), it is important to develop nanomaterials with antimicrobial properties. Persistence and spreading of infections which are caused by MDR microorganisms (bacteria, viruses, fungi and parasites) lead to ineffective treatment in patients. The emergence of a new persistent bacterial strain is the direct consequence of the non-judicial use of antibiotics. Due to the lack of proper medication methods, poor sterilization practices and the inappropriate handling and dealing of hazardous materials, the risk of multiple infections with pathogenic strains is increasing. In recent times, various metal oxide nanomaterials have been engaged as antimicrobial agents to prevent infection with different kinds of pathogenic microorganisms. In this regard, ZnO NPs are one of those materials which have the potential to exert their antimicrobial activity by rupturing microorganism's cell walls through the reactive oxygen species (ROS) and the generation of Zn²⁺.

* Corresponding author: sasiflorence@gmail.com
<https://doi.org/10.15251/JOBM.2022.142.35>

There are numerous methods have been developed in past decade including chemical and physical approaches such as solvothermal synthesis, sol-gel technique, aqueous chemical reduction method to obtain ZnO NP's [5-7]. The chemical synthesis methods are considered more effective due to its ability to synthesis large quantities of ZnO NP's, however the process could be toxic which may harm the environment in the long term. Due to increased awareness towards green synthesis of ZnO NPs led the research community to develop an eco-friendly method using naturally occurring substances such as sugars, vitamins, plant extracts, medicinal roots, fruit extracts and biodegradable polymers. Although biosynthesis of ZnO NP's by various parts of the plants have been reported such as *Pandanus Amaryllifolius* [15], *Azadirachta indica* [16], *Allium sativum* [17] have been reported, the potential of plants as biological materials for the synthesis of nanoparticles is yet to be fully explored. From this point of view, this study aims at the biosynthesis of ZnO nanoflakes from prepared *Pandanus tectorius* leaf extract (PTLE). *Pandanus tectoris* is commonly distributed in the Jazan region which is a southern part of Saudi Arabia. Due to its therapeutic potentials, all parts of the plants are being used from the ancient times for the treatment of headache, rheumatism, cold, flu, epilepsy, leucoderma, ulcers, hepatitis, smallpox, leprosy, syphilis, and even cancer. It also acts as a cardiogenic, antioxidant, dysuric, an aphrodisiac.

Pandanus tectorius leaf extracts are a very promising tool for the facile green synthesis of metal oxide NPs. *Citrus aurantifolia* fruit juice, *Parthenium hysterophorus* leaf extracts, and *Aloe* species extracts have been used in the synthesis of ZnO NPs. The synthesis of ZnO nanoparticles using *Pandanus odorifer* leaf water extract (POLE) has already been reported. The presence of hydroxyl and ketonic groups has been confirmed by FTIR analysis. It is a well-established fact that these functionally active components act as reducing as well as a stabilizing agent during the biosynthesis of metal-based nanoparticles. Recent studies have discovered that plant metabolites such as sugars, terpenoids, phenolic, alkaloids, phenolic acids, and proteins play a significant role in the reduction of metal ions into nanoparticles and in providing stability to nanoparticles.

As a result, it is important to search for a greener, sustainable and environment friendly method is desirable to synthesis ZnO materials for antimicrobial applications. In the present work, PTLE extract has been used to study the effect of structural, morphological and optical properties of ZnO nanostructures. Thus, the synthesis of PTLE assisted ZnO nanoflakes via a facile wet chemical reaction method at room temperature is hereby reported.

2. Experimental work

2.1. Materials and reagents

Analytical grade reagents ($\text{Zn}(\text{CH}_3\text{COO})_2 \cdot 2\text{H}_2\text{O}$) and Sodium Hydroxide (NaOH) were purchased from Merck and used without further purification. Bacterial culture media were purchased from HiMedia (Pvt. Ltd. Mumbai, India). Glassware and plastic consumables were obtained from Asila, Riyadh.

2.2. Preparation of pandanus tectorius leaves extract (PTLE)

Fresh leaves *pandanus tectorius* were collected and washed several times with water to remove dust particles. The extract used for the synthesis of ZnO nanoflakes was prepared by placing 300 g of washed dried fine cut leaves in 100 ml glass beaker along with 90 ml of sterile distilled water. The mixture then was boiled at temperature of 90°C for 90 minutes. The extract was cooled to room temperature and was filtered using filter paper before being stored in a refrigerator for further use.

2.3. Biosynthesis of ZnO NFs

Synthesis was carried out by a simple synthesis method by using zinc acetate [$\text{Zn}(\text{CH}_3\text{COO})_2$] and Sodium Hydroxide (NaOH) as source powders. In a typical synthesis of ZnO nanoflakes, an aqueous solution of 1 M zinc acetate was added to an aqueous solution of 1 M Sodium Hydroxide in a 100 mL beaker, under constant stirring. This was followed by a slow addition of an aqueous solution of PTLE. The mixture was further stirred for 2 h at room

temperature which lead to the formation of a precipitate. The precipitate was washed several times and annealed at 120°C for 3 h followed by filtration.

2.4. Characterization of ZnO NFs

The structure of the dried samples were characterized by X-ray Diffraction(XRD) using X'Per PRO (PANalytical) X-ray Diffractometer using Cu K α radiation of wavelength 1.5406 Å in the scan range 20–80° with a step size of 0.02°.

3. Results and discussion

3.1. Structural studies

XRD pattern of green synthesized ZnO NFs is shown in Fig.1. which represents the diffraction peaks at (100), (002), (101), (110), (103) and (112) planes respectively (PDF#36-1451). The diffracted peaks fit well a wurtzite structure. The crystallite size of ZnO NFs was measured by using Scherer formula and calculated in the range of 20 to 80nm.

The crystalline nature of ZnO NFs is proved with the narrow and solid diffraction peaks, which is consistent with the XRD pattern of ZnO NFs in the present study. There are no peaks are found as crystallographic impurities in the green synthesized ZnO NF. Broadening of XRD peaks not only showed the formation of small nanoflakes, but the effects of PTLE are reflected in nucleation as well as crystalline nuclei growth which is in agreement with some previous reports using *Plectranthus Amboinicus* leaf extract, *Ulva lactuca* seaweed extract, *Lantana aculeate* leaf extract, *Eichhornia crassipes* leaf extract and *Pandanus odorifer* leaf extract (POLE) synthesised ZnO NPs.

The Raman spectrum is one of the essential tools which helps to study the in micro/nanostructure's crystallization, defects and structural disorder. The vibrational properties of the PTLE synthesized ZnO nanoflakes are investigated by using Raman spectra. The optical modes should exist in a wurtzite ZnO according to the group theory as given in equation (1).

$$\Gamma_{\text{opt}} = A_1 + 2B_2 + E_1 + 2E_2 \quad (1)$$

where, A_1 and E_1 modes are two polar branches, which is spitting into two components namely longitudinal optical (LO) and transversal optical (TO) with altered frequencies due to the LO phonons associated macroscopic electric fields. The A_1 , E_1 , and E_2 modes are first order Raman-active modes. Fig. 2 shows the Raman spectra of PTLE synthesized ZnO nanoflakes. The multi phonon scattering modes are presented at 345 and 673 which are assigned to the $3E_{2H}-E_{2L}$ and $2(E_{2H}-E_{2L})$ respectively. An additional peak depicted at about 217 cm^{-1} shows the second order ($2E_{2L}$) phonon mode of the Raman peak.

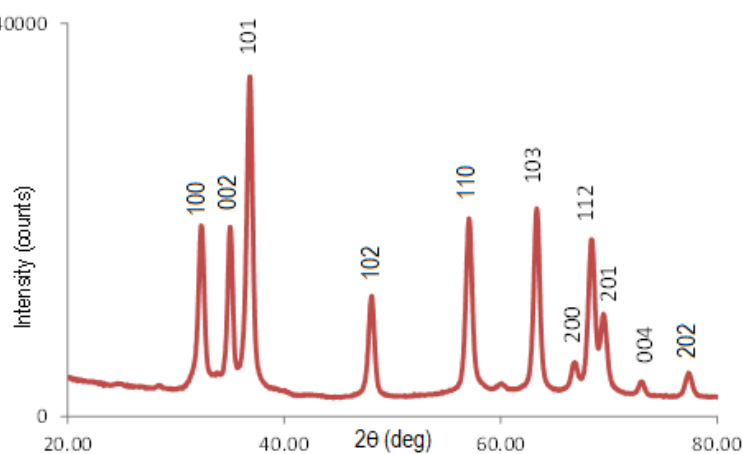


Fig. 1. XRD pattern of green synthesized ZnO NFs.

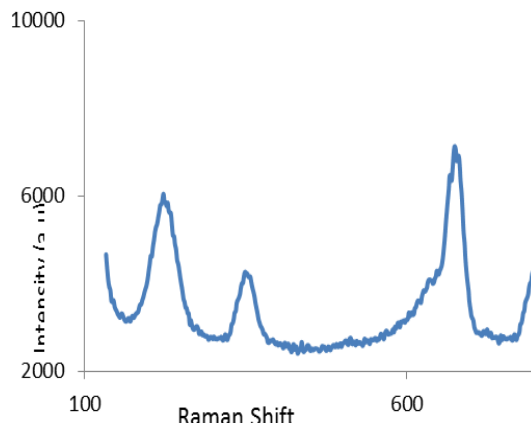


Fig. 2. Raman spectra of green synthesized ZnO NFs.

SEM micrographs of ZnO NFs are shown in Fig. 3 (a&b). SEM micrographs reveal the presence of variable sized PTLE green synthesized ZnO NFs. The transmission emission microscopy measurements also show that the as synthesized samples are square and rectangular flake shaped transparent particles and the size varies from 100-400 nm as illustrated in Fig.3 (c&d). The high and low energy state electron transitions can be probed by the PL spectroscopy which can allow the investigation of the impurities, defects, and bandgaps in semiconductor materials. Fig. 4 shows the room-temperature PL spectra for PTLE synthesized ZnO nanoflakes. The emission spectrum of ZnO nanoflakes was obtained using He:Cd laser as the excitation source with a wavelength of 360 nm. The emission spectrum presents three typical emission bands centered at 455 nm, 483 nm and 548 nm respectively.

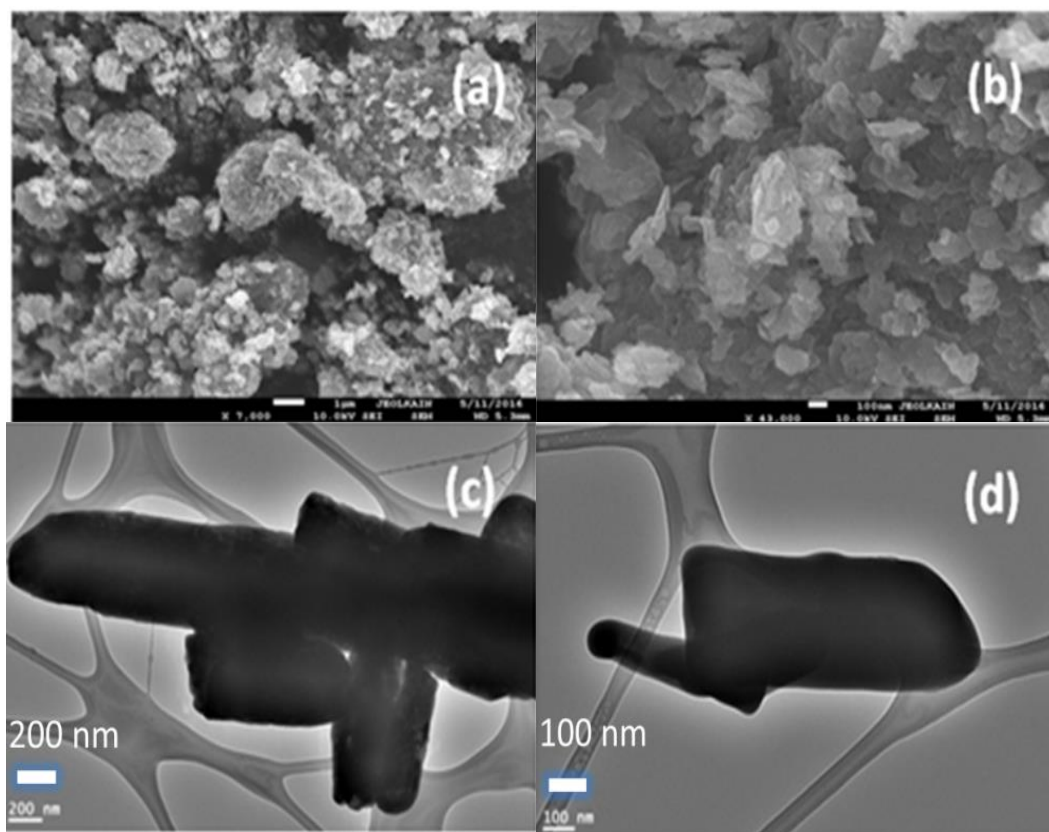


Fig. 3. SEM and TEM pictures of PTLE green synthesized ZnO NFs.

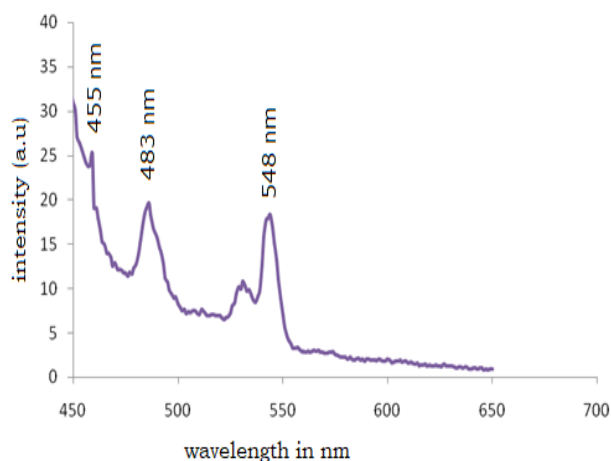


Fig. 4. PL spectra of PTLE green synthesized ZnO NFs.

The first one was an exciton emission band in the UV region which has been caused by the radiative annihilation of excitons whereas the second and third one were the intense bands in the green and blue region of the visible spectrum produced by the radiative recombination of an electron from conduction band and an deeply trapped hole in the bulk of an ZnO particle [17]. Previous research studies show that the metallic solid Zn nanoflakes demonstrate high-intensity emission band centered at 408 nm and a low-intensity broad emission band from 450 to 700 nm [18]. In addition, the visible emission band centered at 548 nm is much prominent than that centered at other two peaks, as shown Fig.4. Overall, ZnO nanoflakes synthesized using PTLE have good and effective visible-light emissions at room temperature, so they are all potential candidates for use in optoelectronic nanodevices, such as light-emitting diodes and laser diodes.

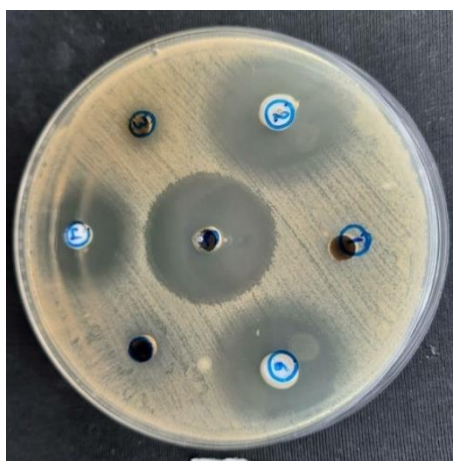


Fig. 5. Antibacterial activity of PTLE green synthesized ZnO NFs.

Fig. 5 shows the *antibacterial activity* of PTLE synthesized ZnO nanoflakes which shows excellent antimicrobial activity against *Bacillus subtilis* which is a Gram-positive . Nutrient agar media plates were used for zone inhibition tests. The plate contained a well loaded with the ZnO nanoflakes, which diffused into the surrounding media and prevented bacterial growth in a zone around the well. We observed excellent zone inhibition at 24 mm and 25 mm against *B. subtilis*.

4. Conclusion

PTLE assisted ZnO nanoflakes have been synthesized by a simple green synthesis method using pandanus tectorius leaves extract. XRD, SEM, FT Raman and PL optical studies revealed the uniform, polycrystalline, wurtzite structure with flake shaped morphological structure of ZnO NFs. The SEM and TEM images reveal the formation of ZnO nanoflakes. The hexagonal wurtzite structure has been predicted from XRD results. Strong blue absorption and the enhanced luminescence property with respect to bulk have been observed from PL studies. These ZnO nanoflakes are well known to possess optical, photoluminescent properties and shows excellent antibacterial properties.

Acknowledgements

The authors (S.S.Florence & C.Manna) extend their appreciation to the Deputyship for Research & Innovation, Ministry of Education in Saudi Arabia for funding this research work through the Project number: RUP-3.

References

1. J.F. Balch, P.A. Balch, Nutritional Healing, Garden City Park, NY 1997; <https://doi.org/10.7901/2169-3358-1997-1-944>
2. S. Livine, G. Myhre, G. Smith, J. Bums, Equine Pract 1982;4:16.
3. A. Umar, A. Al-Hajry, R. Ahmad, S.G. Ansari, M.S. Al-Assiria, H. Algarni, Dalton Trans. 2015;44:21081; <https://doi.org/10.1039/C5DT03364K>
4. Yury Gogotsi, Nanomaterials Handbook, Taylor& Francis 2006; <https://doi.org/10.1201/9781420004014>
5. Chen Y, Bagnall DM, Hang-jun Koh, Ki-tae Park, Hiraga K, Zhu Z, et al. J Appl. Phys 1998;84:3912; <https://doi.org/10.1063/1.368595>
6. Schmidt-Mende L, MacManus-Driscoll JL. Mater Today 2007;10:40; [https://doi.org/10.1016/S1369-7021\(07\)70078-0](https://doi.org/10.1016/S1369-7021(07)70078-0)
7. Savaloni H, Gholipour-Shahraki M, Player MA. J Phys D Appl Phys 2006;39:2231; <https://doi.org/10.1088/0022-3727/39/10/036>
8. Pearton SJ, Norton DP, Ip K, Heo YW, Steiner T. Prog Mater Sci 2005;50:293; <https://doi.org/10.1016/j.pmatsci.2004.04.001>
9. Özgür U, Alivov YI, Liu C, Teke A, Reshchikov MA, Dog˘an S, et al. J Appl Phys 2005;98:041301; <https://doi.org/10.1063/1.1992666>
10. Florence SS, John R, Arockiasamy DL, Umadevi M. Mater Lett 2012;86:129; <https://doi.org/10.1016/j.matlet.2012.07.057>
11. Florence SS, Umadevi M, John R, Arockiasamy DL. Mater Lett 2013;108:5; <https://doi.org/10.1016/j.matlet.2013.06.061>
12. Florence SS, Umadevi M, John R, Arockiasamy DL. Mater Lett 2014;115:34; <https://doi.org/10.1016/j.matlet.2013.10.028>
13. Florence SS, Hajer Adam, Chadlia Manna, Nurdogan Can. AIP Proceedings 2018; 020020:1.
14. Florence SS, Nurdogan Can. Results in Physics 2018;10:1731 <https://doi.org/10.1016/j.rinp.2018.05.041>
15. Calleja J M and Cardona M Phys. Rev. B 1977;16:3753; <https://doi.org/10.1103/PhysRevB.16.3753>
16. Cusco R, Alarc'on-Llad'o E, Ib ' a˜nez J, Art'us L, Jim'enez J, Wang B and Callahan M J Phys. Rev. B 2007;75:165202.
17. S. Music, A. Saric and S. Popovic, Jour of Alloys and Comp 2008;448:277; <https://doi.org/10.1016/j.jallcom.2006.10.021>

18. Jin-Han Lin, Ranjit A. Patil, Rupesh S. Devan, Zhe-An Liu, Yi-Ping Wang, Ching-Hwa Ho, Yung Liou & Yuan-Ron Ma, *Nature, scientific reports* 2014; 4:6967.